arXiv:cond-mat/0206147v2 20 Aug 2002

Pair distribution function of the spin-polarized electron gas: A first-principles analytic model for all uniform densities

Paola Gori-Giorgi[1] and John P. Perdew[2]
[1] *INFM Center for Statistical Mechanics and Complexity, and Dipartimento di Fisica, Università di Roma "La Sapienza", Piazzale A. Moro 2, 00185 Rome, Italy*
[2] *Department of Physics and Quantum Theory Group, Tulane University, New Orleans, Louisiana 70118 USA*
(Dated: March 22, 2022)

We construct analytic formulas that represent the coupling-constant-averaged pair distribution function $\overline{g}_{xc}(r_s,\zeta,k_F u)$ of a three-dimensional non-relativistic ground-state electron gas constrained to a uniform density with density parameter $r_s=(9\pi/4)^{1/3}/k_F$ and relative spin polarization ζ over the whole range $0<r_s<\infty$ and $-1<\zeta<1$, with energetically-unimportant long range ($u\to\infty$) oscillations averaged out. The pair distribution function g_{xc} at the physical coupling constant is then given by differentiation with respect to r_s. Our formulas are constructed using *only* known theoretical constraints plus the correlation energy $\epsilon_c(r_s,\zeta)$, and accurately reproduce the g_{xc} of the Quantum Monte Carlo method and of the fluctuation-dissipation theorem with the Richardson-Ashcroft dynamical local-field factor. Our g_{xc} is correct even in the high-density ($r_s\to 0$) and low-density ($r_s\to\infty$) limits. When the spin resolution of ϵ_c into $\uparrow\uparrow$, $\downarrow\downarrow$, and $\uparrow\downarrow$ contributions is known, as it is in the high- and low-density limits, our formulas also yield the spin resolution of g_{xc}. Because of these features, our formulas may be useful for the construction of density functionals for non-uniform systems. We also analyze the kinetic energy of correlation into contributions from density fluctuations of various wavevectors. The exchange and long-range correlation parts of our $\overline{g}_{xc}(r_s,\zeta,k_F u)-1$ are analytically Fourier-transformable, so that the static structure factor $\overline{S}_{xc}(r_s,\zeta,k/k_F)$ is easily evaluated.

I. INTRODUCTION, DEFINITIONS, AND OUTLINE

The exchange-correlation pair-distribution function $g_{xc}(\mathbf{r},\mathbf{r}')$ of an N-electron system is defined as

$$g_{xc}(\mathbf{r},\mathbf{r}')=\frac{N(N-1)}{n(\mathbf{r})n(\mathbf{r}')}\int|\Psi(\mathbf{r},\mathbf{r}',\mathbf{r}_3...\mathbf{r}_N)|^2 d\mathbf{r}_3...d\mathbf{r}_N, \tag{1}$$

where $n(\mathbf{r})$ is the electron density and Ψ is the many-body wavefunction. Its coupling-constant average $\overline{g}_{xc}(\mathbf{r},\mathbf{r}')$ is equal (in the Hartree units used throughout) to

$$\overline{g}_{xc}(\mathbf{r},\mathbf{r}')=\int_0^1 d\lambda\, g^{\lambda}_{xc}(\mathbf{r},\mathbf{r}'), \tag{2}$$

where $g^{\lambda}_{xc}(\mathbf{r},\mathbf{r}')$ is the pair-distribution function when the electron-electron interaction is $\lambda/|\mathbf{r}-\mathbf{r}'|$ and the density is held fixed at the physical or $\lambda=1$ density. The coupling-constant averaged $\overline{g}_{xc}$ plays a crucial role in density functional theory, since it can account for the kinetic energy of correlation.[1] In fact, $n(\mathbf{r}')\,[\overline{g}_{xc}(\mathbf{r},\mathbf{r}')-1]$ is the density at $\mathbf{r}'$ of the exchange-correlation hole around an electron at $\mathbf{r}$.

In the uniform electron gas, $n(\mathbf{r})=n$ and $g_{xc}(\mathbf{r},\mathbf{r}')$ only depends on $u=|\mathbf{r}-\mathbf{r}'|$, and parametrically on the density parameter $r_s=(3/4\pi n)^{1/3}$ and on the spin-polarization $\zeta=(N_\uparrow-N_\downarrow)/N$. The coupling-constant average is in this case[2] equivalent to an average over r_s:

$$\overline{g}_{xc}(r_s,\zeta,k_F u)=\frac{1}{r_s}\int_0^{r_s} g_{xc}(r_s',\zeta,k_F u)\,dr_s', \tag{3}$$

where $k_F=(9\pi/4)^{1/3}/r_s$ is the Fermi wavevector. Clearly then

$$g_{xc}(r_s,\zeta,k_F u)=\frac{\partial}{\partial r_s}\left[r_s\,\overline{g}_{xc}(r_s,\zeta,y)\right]\Big|_{y=k_F u}, \tag{4}$$

and

$$g^{\lambda}_{xc}(r_s,\zeta,k_F u)=g_{xc}(\lambda r_s,\zeta,k_F u). \tag{5}$$

The high-density ($r_s\to 0$) limit is the weak-interaction limit in which the kinetic energy dominates. Relativistic effects are important for $r_s\lesssim 0.01$. The low-density ($r_s\to\infty$) limit is the strong-interaction limit in which the Coulomb potential energy dominates. For $r_s\gtrsim 100$, the true ground-state density is not uniform,[3] but there is still a wavefunction that achieves the lowest energy of all those constrained to a given uniform density.

The electron gas of uniform density is a paradigm of the density functional theory[1] for real, non-uniform electronic systems. The exchange-correlation energy of the uniform gas is the input to the local spin density approximation, while the coupling-constant-averaged pair-distribution function is an input to the derivation of gradient-corrected functionals,[4,5] to the construction of the corresponding system-averaged exchange-correlation hole of a non-uniform density,[5] and to the implementation of the fully-nonlocal weighted density approximation.[6,7,8] We hope that our improved analytic model will be useful for these purposes, and also for the construction of new and more accurate functionals. In particular, the spin-resolved version of our model, when fully developed, could bring useful new information for the construction of functionals. Indeed, simple hypotheses for the spin resolution have already been

used to construct several correlation functionals.[9,10] The uniform-gas g_{xc} is also relevant to density matrix functional theory.[11]

The static structure factor $S_{xc}(r_s,\zeta,k/k_F)$ is the Fourier transform

$$S_{xc}(r_s,\zeta,k/k_F) = 1+\frac{4}{3\pi}\int_0^\infty [g_{xc}(r_s,\zeta,k_F u)-1]\times (k_F u)^2\frac{\sin ku}{ku}\,d(k_F u), \quad (6)$$

and its coupling-constant average $\overline{S}_{xc}$ is obtained by changing g_{xc} into $\overline{g}_{xc}$ in Eq. (6). Usually g_{xc} and consequently $\overline{g}_{xc}$, S_{xc}, and $\overline{S}_{xc}$ are divided into exchange and correlation contributions:

$$g_{xc}(r_s,\zeta,k_F u) = g_x(\zeta,k_F u)+g_c(r_s,\zeta,k_F u), \quad (7)$$

where the exchange function g_x is obtained by putting a Slater determinant of Kohn-Sham orbitals (or of Hartree-Fock orbitals) into Eq. (1). For a uniform electron gas, both Kohn-Sham and Hartree-Fock orbitals are plane waves, and g_x is a simple function of $k_F u$. The exchange-only pair-distribution function does not depend explicitly on r_s, so that $\overline{g}_x = g_x$: the explicit dependence on r_s only appears when Coulomb repulsion is taken into account in the wavefuction.

Both g_x and g_c have long-range oscillations. At high densities, these are Friedel oscillations; at low densities, they represent the incipience of Wigner-crystal order within the liquid phase of uniform density. These oscillations are energetically unimportant in the following sense:[2] A model which omits them but is constrained to have the same energy integral can correctly describe the short-range correlation while averaging out the oscillations of the long-range correlation. The energetic unimportance of the oscillations is probably a consequence of the long-range and "softness" of the Coulomb interaction.

Available analytic models[2,12] of g_c and $\overline{g}_c$ for the uniform electron gas break down at high[13,14] ($r_s \lesssim 0.1$) and low ($r_s > 10$) densities. In this paper, we present a new model for the nonoscillatory part of $\overline{g}_c$ (and hence g_c) which fulfills most of the known exact properties and is valid over the whole ($0 < r_s < \infty$) density range and for all spin polarizations ζ. Our model is built up by interpolating between the short-range part recently computed in Ref. 15 and the long-range nonoscillatory part which is exactly given by the random-phase approximation[16] (RPA). Exact small-u and large-u expansions are recovered up to higher orders with respect to currently available models.[2,12] All the parameters which appear in our interpolation scheme are fixed by exact conditions. We also build up a new nonoscillatory exchange g_x which fulfills exact short-range and long-range properties up to the same order as our $\overline{g}_c$ does.

The paper is organized as follows. In Sec. II, we list the known exact properties of g_{xc} and $\overline{g}_{xc}$, and the major limitations of the models of Refs. 2 and 12. We then present our nonoscillatory model for exchange (Sec. III) and for correlation (Sec. IV). In Sec. V, we discuss our results for exchange and correlation over the whole density range. At metallic densities, we compare our analytic model with the available Quantum Monte Carlo (QMC) data,[3,17] finding fair agreement (Fig. 3). We also computed g_c corresponding to the dynamic local-field factors of Richardson and Ashcroft[18] (RA), in order to see better how our model averages out the long-range oscillations (currently not available from QMC). In this way, we are also able to show the effect of a dynamic local-field factor on the long-range oscillations, by comparing the RA result with the RPA (corresponding to zero local-field factor) long-range g_c (Fig. 4). At high density, we find that our model is in very good agreement with exact calculations[13,19] (Fig. 5), and at low density it does not break down and shows the expected ζ dependence (Fig. 1). We also compare (Fig. 6) our model with previous models,[2,12] and discuss the qualitative effects of correlation (Fig. 7). In Sec. VI, we discuss how to extend our scheme to the spin-resolved ($\uparrow\uparrow$, $\downarrow\downarrow$ and $\uparrow\downarrow$) pair-distribution functions. The wavevector analysis of the kinetic energy of correlation corresponding to our S_c and $\overline{S}_c$ is presented in Sec. VII. Section VIII is devoted to conclusions and perspectives.

II. EXACT PROPERTIES, AND LIMITATIONS OF PREVIOUS MODELS

We list below most of the known exact properties of g_{xc} and $\overline{g}_{xc}$ for the 3D uniform electron gas. Equation (1) implies the positivity constraint $g_{xc} \geq 0$ and the particle-conservation sum rule, which can be divided into exchange and correlation,

$$\int_0^\infty du\, 4\pi u^2 n\,(g_x-1) = -1 \quad (8)$$

$$\int_0^\infty du\, 4\pi u^2 n\, g_c = \int_0^\infty du\, 4\pi u^2 n\,\overline{g}_c = 0. \quad (9)$$

With the Coulomb interaction $1/u$, the exchange function g_x, the correlation function g_c, and its coupling-constant averaged $\overline{g}_c$ integrate to the exchange energy ϵ_x, to the potential energy of correlation v_c, and to the correlation energy ϵ_c respectively,

$$\frac{1}{2}\int_0^\infty du\, 4\pi u^2 \frac{1}{u} n\,(g_x-1) = \epsilon_x(r_s,\zeta), \quad (10)$$

$$\frac{1}{2}\int_0^\infty du\, 4\pi u^2 \frac{1}{u} n\, g_c = v_c(r_s,\zeta) \quad (11)$$

$$\frac{1}{2}\int_0^\infty du\, 4\pi u^2 \frac{1}{u} n\,\overline{g}_c = \epsilon_c(r_s,\zeta). \quad (12)$$

For further discussion of the exchange hole density $n\,(g_x-1)$ surrounding an electron, the correlation hole density $n\,g_c$, and the generalization of Eqs. (8)-(12) to nonuniform densities, see Refs. 6 and 20.

The short-range behavior of g_{xc} is determined by the $1/u$ Coulomb repulsion, which gives rise to the cusp condition[21]

$$\frac{dg_{xc}}{du}\Big|_{u=0} = g_{xc}\Big|_{u=0}. \tag{13}$$

The function $\overline{g}_{xc}$ satisfies a modified cusp condition[2,15] which can be derived from Eqs. (3) and (13). A quite accurate estimate of the r_s and ζ dependence of the short-range expansion coefficients of g_{xc} and $\overline{g}_{xc}$ has been recently obtained by solving a scattering problem in a screened Coulomb potential which describes the effective electron-electron interaction in a uniform electron gas – the extended solution[15] of the Overhauser model.[22] (Classical electrons at zero temperature would have $g_{xc}|_{u=0} = 0$, but nonzero values have a nondivergent potential-energy cost according to Eq. (11) and for quantum mechanical electrons lower the kinetic energy associated with the swerving motion needed to keep two electrons from colliding. Thus the right-hand side of Eq. (13) is nonzero, except in the low-density limit. It is similarly nonzero for a gas of classical electrons at an elevated temperature.[23])

The long-range part of the nonoscillatory g_{xc} corresponds to the small-k behavior of the static structure factor, which is determined by the plasmon contribution, proportional to k^2, and by the single-pair and multipair quasiparticle-quasihole excitation contributions, proportional to k^5 and k^4 respectively,[24,25]

$$S_{xc}(r_s, \zeta, k \to 0) = \frac{k^2}{2\omega_p(r_s)} + O(k^4), \tag{14}$$

where $\omega_p(r_s) = \sqrt{3/r_s^3}$ is the plasma frequency. Equation (14) is called the plasmon sum rule. There is no k^3 term in the small-k expansion[27] of S_{xc}. Since, when $k \to 0$, the exchange-only static structure factor S_x is equal to

$$S_x(\zeta, k \to 0) = \frac{3}{8}\left[(1+\zeta)^{2/3} + (1-\zeta)^{2/3}\right]\frac{k}{k_F} - \frac{k^3}{16k_F^3}, \tag{15}$$

there must be a linear term and a cubic term in the small-k expansion of the correlation static structure factor S_c which cancel with the exchange. In real space, these terms correspond to long-range tails $\propto u^{-4}$ and $\propto u^{-6}$ respectively.[2,26] The nonoscillatory exchange-correlation pair-distribution function has a long-range tail[12,26] $\propto u^{-8}$. As for more general densities, the exchange-correlation hole is more localized around its electron than the exchange hole (and thus better described by local or semi-local approximations for non-uniform densities). The high-density limit of the random-phase approximation (RPA) exactly describes[16] the nonoscillatory long-range part of g_{xc}, recovering Eq. (14) through order k^2. The absence of the k^3 term in the small-k expansion of S_{xc} was demonstrated for the $\zeta = 0$ gas by using exact frequency-moment sum rules.[27] The same arguments should hold for the $\zeta \neq 0$ gas. Notice that the cancellation of the k^3 terms is obtained from beyond-RPA considerations.[27]

Armed with these exact constraints, we can discuss the strengths and weaknesses of previous analytic models, which unlike our present model break down[13,14] outside the metallic density range $1 \lesssim r_s \lesssim 10$.

The Perdew-Wang model[2] was largely based on first principles, plus limited fitting to Quantum Monte Carlo data. This model introduced the high-density limit of the RPA as the long-range component of g_{xc}. But that limit was modelled crudely, leading to violation of the particle-conservation sum rule (and thus to failure for $r_s \lesssim 0.1$). The model did not incorporate the plasmon sum rule, and produced an incorrect u^{-5} nonoscillatory long-range limit for g_{xc}. The positivity constraint was violated at low densities, a problem evaded by switching over to a different analytic form for $r_s > 10$. In this model, the spin resolution of g_{xc}, even in its revised form,[14] is less reliable than the total g_{xc}.

The model of Gori-Giorgi, Sacchetti, and Bachelet[12] was based upon extensive fitting to spin-resolved Quantum Monte Carlo data for $\zeta = 0$, and did not address nonzero ζ. Their model for g_{xc}, unlike that of Perdew and Wang, was analytically Fourier-transformable to S_{xc}. It incorporated the particle-conservation and plasmon sum rules, and the correct u^{-8} long-range limit for g_{xc}, but did not build in the important high-density limit of the RPA for large u, leading to failure for $r_s \ll 0.8$. Moreover, small-u errors of the Monte Carlo data were transferred into the model.[15]

III. NONOSCILLATORY EXCHANGE HOLE

We present here our nonoscillatory model for the exchange hole. This new model satisfies exact short-range and long-range conditions up to the same order as our correlation-hole model (Sec. IV) does.

The exact exchange-only pair-distribution function for the uniform gas is

$$\begin{aligned} g_x(\zeta, k_F u) &= 1 + \tfrac{1}{2}\{(1+\zeta)^2 J[(1+\zeta)^{1/3} k_F u] \\ &\quad + (1-\zeta)^2 J[(1-\zeta)^{1/3} k_F u]\}, \end{aligned} \tag{16}$$

where

$$J(y) = -\frac{9}{2}\left(\frac{\sin y - y\cos y}{y^3}\right)^2. \tag{17}$$

Our nonoscillatory $\langle J(y)\rangle$ is parametrized as

$$\begin{aligned} \langle J(y)\rangle &= \frac{-9}{4y^4}\Big[1 - e^{-A_x y^2}\Big(1 + A_x y^2 + \frac{A_x^2 y^4}{2} + \frac{A_x^3 y^6}{3!}\Big)\Big] \\ &\quad + e^{-D_x y^2}(B_x + C_x y^2 + E_x y^4 + F_x y^6). \end{aligned} \tag{18}$$

This model is similar in spirit, but not in detail, to those of Refs. 2 and 28. The first term of Eq. (18) achieves the

correct average long-range behavior $-\frac{9}{4}y^{-4}$ as $y \to \infty$, and is damped out at small y by the first square bracket which varies from y^8 as $y \to 0$ to 1 as $y \to \infty$. The second term then builds in the correct small-y behavior. The Gaussians smoothly blend the two terms, but are not motivated by any physical model. The analytic forms and linear parameters in Eq. (18) are convenient for constraint satisfaction. The separation into long-range and short-range parts, although somewhat arbitrary, could be useful for the construction of new density functionals. The spherical Fourier transform of $\langle J(y)\rangle$,

$$\tilde{J}(k) = \int_0^\infty \langle J(y)\rangle y^2 \frac{\sin(ky)}{ky}\, dy, \tag{19}$$

is also analytic and is reported in Appendix A. The large-y expansion of Eq. (18) is

$$\langle J(y\to\infty)\rangle = -\tfrac{9}{4}y^{-4} + O(e^{-y^2}), \tag{20}$$

while the nonoscillatory average of the exact $J(y)$ also contains a $-\frac{9}{4}y^{-6}$ term (and no other long-range term). Such a term was included in the models of Refs. 2 and 28, but with a coefficient wrong in both sign and magnitude. As explained in Sec. II, the exact nonoscillatory correlation hole has long-range terms y^{-4} and y^{-6} which exactly cancel with the exchange,[12,26,27] so that the exact nonoscillatory exchange-correlation hole has a long-range tail[12,26] $\propto u^{-8}$ which is purely correlation. However, as detailed in Sec. IV A, our nonoscillatory correlation-hole model is built without a u^{-6} long-range term, since this choice preserves a simple and useful scaling. We have thus also set the y^{-6} term to zero in our nonoscillatory exchange-hole model, in order to have an exchange-correlation hole with the exact u^{-8} long-range behavior.

The six parameters A_x through F_x are fixed by requiring that (i) the particle-conservation sum rule is fulfilled, (ii) our g_x gives zero contribution to the plasmon sum rule, (iii) our g_x recovers the exact exchange energy, (iv) our g_x is exact at $u = 0$ in obedience to the Pauli principle in real space (two electrons of parallel spin cannot come together, since the antisymmetry of the wavefunction makes this probability vanish), (v) our g_x has the exact second derivative at $u = 0$, and (vi) the information entropy $\mathcal{S}[-J(y)]$,

$$\mathcal{S}[-J(y)] = \int_0^\infty dy\, 4\pi y^2 J(y) \ln[-J(y)], \tag{21}$$

is maximized.[28,29] $\mathcal{S}$ of Eq. (21) is not a thermodynamic entropy but a mathematical one whose maximization ensures that the analytic $J(y)$ has no structure beyond that imposed by the exact constraints used to construct it. The parameter values are $A_x = 0.77$, $B_x = -0.5$, $C_x = -0.08016859$, $D_x = 0.3603372$, $E_x = 0.009289483$, and $F_x = -0.0001814552$.

Our nonoscillatory model g_x is compared with the exact exchange at $\zeta = 0$ and $\zeta = 1$ in the upper panel of Fig. 1. In the first panel of Fig. 4, the exchange hole

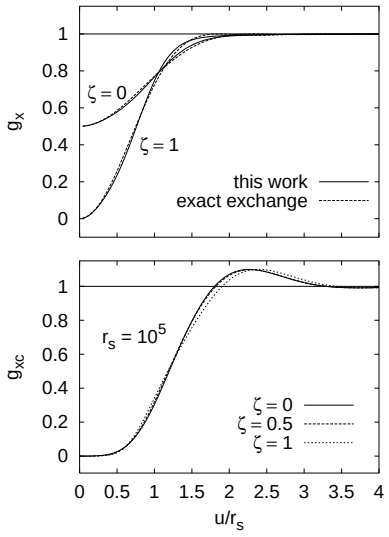


FIG. 1: Upper panel: our nonsoscillatory model for exchange in the uniform electron gas is compared with the exact Hartree-Fock curve. Note that g_x is the $r_s \to 0$ limit of g_{xc}. Lower panel: low-density limit of our analytic model for the exchange-correlation pair-distribution function of the uniform gas. In this limit, the model g_{xc} is almost exactly independent of the relative spin polarization ζ.

$g_x - 1$ is multiplied by $(u/r_s)^4$ in order to show how our model (solid line) averages out the oscillations of the exact exchange hole (dashed line).

IV. NONOSCILLATORY CORRELATION HOLE

Following Perdew and Wang,[2] we write the nonoscillatory part of the correlation hole as the sum of a long-range part and a short-range part, somewhat as in Eq. (18):

$$\langle \overline{g}_c(r_s,\zeta,k_F u)\rangle = \frac{\phi^3 r_s}{\kappa}\frac{\overline{f}_1(v)}{(k_F u)^2}\Big[1 - e^{-d\,x^2}\Big(1 + d\,x^2 + \frac{d^2}{2}\,x^4\Big)\Big] + e^{-d\,x^2}\sum_{n=1}^{6} c_n\, x^{n-1}, \tag{22}$$

where $\kappa = (4/3\pi)(9\pi/4)^{1/3}$, $\phi = [(1+\zeta)^{2/3}+(1-\zeta)^{2/3}]/2$, $x = k_F u/\phi$, and $v = \phi\kappa\sqrt{r_s}k_F u$. The six linear parameters c_n depend on both r_s and ζ, while the nonlinear parameter d only depends on ζ.

The first term in the r.h.s. of Eq. (22) is the long-range part of our $\overline{g}_c$: the function $\overline{f}_1(v)$ is a new parametrization (see Sec. IV A) of the RPA limit found by Wang and Perdew[16] and displayed in Fig. 2 of Ref. 2. We multiplied $\overline{f}_1(v)/(k_F u)^2$ by a cutoff function which cancels its small-u contributions, so that the long-range part of our $\overline{g}_c$ vanishes through order u^4 and does not interfere with the short-range part.

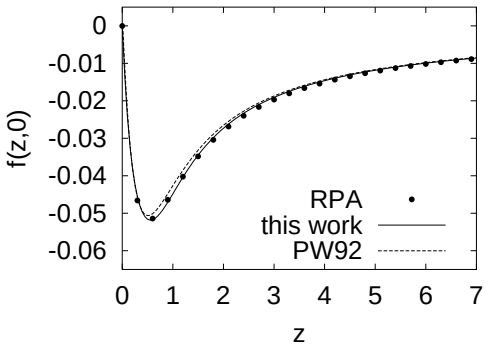


FIG. 2: The function $f(z,0)$ given in Ref. 16. The exact calculation (RPA) is compared with the present parametrization and with the one of Perdew and Wang[2] (PW92).

For modeling the short-range part, corresponding to the last term in the r.h.s. of Eq. (22), we use our recent results obtained by solving the Overhauser model,[15] which allow us to fix the r_s and ζ dependence of the linear parameters c_1, c_2 and c_3 (Sec. IV B). We then use the remaining three linear parameters, c_4, c_5 and c_6, to fulfill the particle-conservation sum rule and the plasmon sum rule, and to recover the "exact" correlation energy (Sec. IV C). Finally, the nonlinear parameter $d(\zeta)$, which determines the "mixing" of long-range and short-range contributions, is fixed by imposing the positivity constraint on g_{xc} when $r_s \to \infty$ (Sec. IV D).

A. Long-range part

As discussed in Refs. 16 and 2, the long-range ($u \to \infty$) part of the nonoscillatory correlation hole can be obtained from the random-phase approximation by computing its $r_s \to 0$ limit. One finds

$$n\langle \overline{g}_c(r_s,\zeta,k_F u)\rangle \to \phi^3(\phi k_s)^2 \frac{\overline{f}_1(v)}{4\pi v^2}, \qquad (23)$$

where k_s is the Thomas-Fermi screening wave vector, $k_s = \kappa\sqrt{r_s}k_F$. The function $\overline{f}_1(v)$ is the spherical Fourier transform of the function $f(z,0)$ given by Eqs. (29), (34) and (36) of Ref. 16,

$$\overline{f}_1(v) = 2v^2 \int_0^\infty dz\, z^2\, f(z,0)\, \frac{\sin(vz)}{vz}, \qquad (24)$$

where $z = k/\phi k_s$ is the proper scaled variable in reciprocal space. The small- and large-z expansion of $f(z,0)$ is

$$f(z\to 0,0) \;=\; -\tfrac{3}{\pi^2}z + \tfrac{4\sqrt{3}}{\pi^2}z^2 + O(z^3) \qquad (25)$$

$$f(z\to \infty,0) \;=\; -\tfrac{2(1-\ln 2)}{\pi^2}z^{-1} + O(z^{-2}). \qquad (26)$$

Equation (26) gives the high-density limit of the corresponding correlation energy,

$$\epsilon_c(r_s\to 0,\zeta) = \tfrac{(1-\ln 2)}{\pi^2}\phi(\zeta)^3 \ln r_s + O(r_s^0), \qquad (27)$$

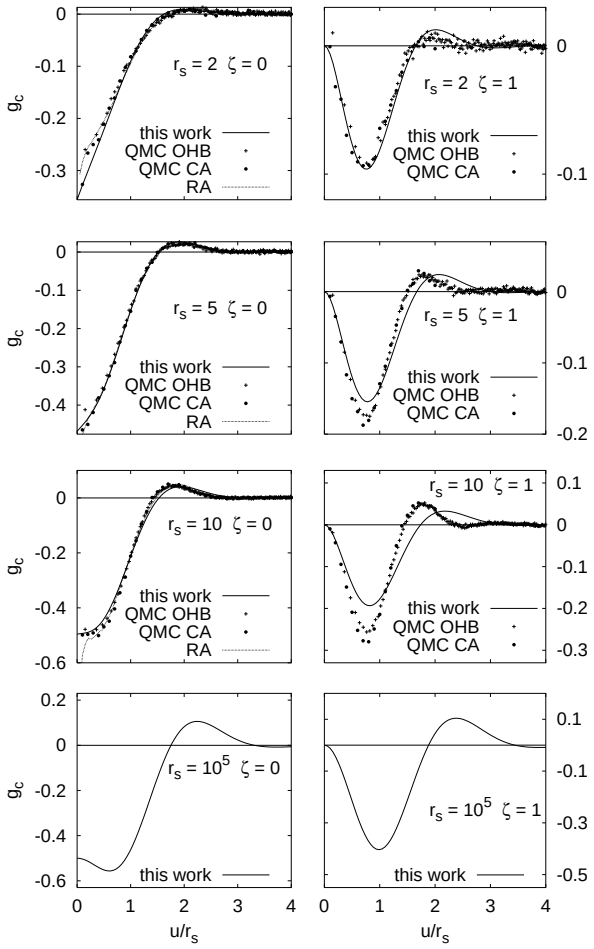


FIG. 3: Coulomb correlation contribution g_c to the pair-distribution function g_{xc} for the uniform electron gas for the paramagnetic ($\zeta = 0$) and ferromagnetic ($\zeta = 1$) state. Our new analytic model is compared with the Diffusion Quantum Monte Carlo results of Ortiz, Harris, and Ballone[17] (OHB), and of Ceperley and Alder[3] (CA). The pair-correlation function corresponding to the local-field-factor model of Richardson and Ashcroft[18] (RA) is also shown. In the two bottom panels, the low-density limit of our g_c is reported.

which is exact at $\zeta = 0$ and 1, but is slightly different from the exact result for $0 < \zeta < 1$ (see Refs. 2 and 16 for further details). The small-z expansion of $f(z,0)$, Eq. (25), fulfills the particle-conservation sum rule [$f(z=0,0) = 0$], contains a linear term which cancels with the exchange (and corresponds to a long-range tail $\propto u^{-4}$ in real space, see Sec. II), and fulfills the plasmon sum rule [exact z^2 coefficient, see Eq. (14)]. The z^3 term in Eq. (25), if it does not vanish, produces a u^{-6} contribution to the correlation hole at large u.

As said in Secs. II and III, the long-range ($u \to \infty$) nonoscillatory behavior of the exact exchange hole contains u^{-4} and u^{-6} contributions which are cancelled[12,26,27] by similar contributions to the exact correlation hole. When we use the high-density limit of Eq. (23) for the long-range part of the correlation hole, we automatically achieve cancellation of the u^{-4} terms.

But to cancel the u^{-6} terms in $g_x - 1$, we would have to replace $\overline{f}_1(v)/v^2$ in Eq. (23) by $\overline{f}_1(v)/v^2 + r_s\phi h(r_s, \zeta, v)$, where $\overline{f}_1(v)/v^2$ has no v^{-6} contribution and h is proportional to v^{-6} with no r_s or ζ dependence at large v. The extra term $r_s\phi h$ vanishes in the high-density limit for a given v, and is unknown. Since we want to keep for our $\overline{g}_c$ the simple form of Eq. (22), but we also want to have the correct long-range behavior ($\propto u^{-8}$) for $\overline{g}_{xc}$, we decided simply to set the u^{-6} terms to zero in both our exchange (Sec. III) and correlation-hole models. Figures 3 and 4 do not suggest that this choice introduces any significant error into our models for the separate exchange and correlation holes.

We thus parametrize $\overline{f}_1(v)$ as follows

$$\overline{f}_1(v) = \frac{a_0 + b_2 v + a_1 v^2 + a_2 v^4 + a_3 v^6}{(v^2 + b^2)^4}. \qquad (28)$$

With respect to the parametrization given by Perdew and Wang,[2] our Eq. (28) has the advantage that it is analytically Fourier-transformable (see Appendix B), so that the particle-conservation sum rule and the plasmon sum rule can be easily imposed. (They are not fulfilled by the Perdew and Wang[2] parametrization). After imposing on our $\overline{f}_1(v)$ all the exact properties plus the vanishing of the z^3 term in Eq. (25), we are left with one free parameter, b, which is fixed by a best fit to our RPA data.[16] All the parameter values are reported in Appendix B. The function $f(z, 0)$ corresponding to our parametrization [see Eq. (B1)] is compared in Fig. 2 with the RPA result and with the Fourier transform of the Perdew and Wang[2] (PW92) $\overline{f}_1(v)$.

B. Short-range part

Our $\overline{g}_c$ has the small-u expansion

$$\langle \overline{g}_c \rangle = c_1 + c_2 \frac{k_F u}{\phi} + (-c_1 d + c_3) \left(\frac{k_F u}{\phi} \right)^2 + O(u^3). \qquad (29)$$

In order to recover the short-range behavior obtained by solving the Overhauser model,[15] we require

$$c_1 = \frac{(1-\zeta^2)}{2} \left[\overline{a}_0^{\uparrow\downarrow}(r_s^{\uparrow\downarrow}) - 1 \right] \qquad (30)$$

$$c_2 = \phi \left(\frac{4}{9\pi} \right)^{1/3} \frac{(1-\zeta^2)}{2} \frac{[(1+\zeta)^{1/3} + (1-\zeta)^{1/3}]}{2} \overline{a}_1^{\uparrow\downarrow}(r_s^{\uparrow\downarrow}) \qquad (31)$$

$$c_3 = \phi^2 \left[\left(\frac{4}{9\pi} \right)^{2/3} \overline{a}_2(r_s, \zeta) - \frac{(1+\zeta)^{8/3} + (1-\zeta)^{8/3}}{20} \right] + \\ + c_1 d, \qquad (32)$$

where $r_s^{\uparrow\downarrow} = 2r_s/[(1+\zeta)^{1/3} + (1-\zeta)^{1/3}]$, and $\overline{a}_0^{\uparrow\downarrow}$, $\overline{a}_1^{\uparrow\downarrow}$ and $\overline{a}_2(r_s, \zeta)$ are given by Eqs. (36), (37) and (46) of Ref. 15. In this way, the modified cusp condition is exactly satisfied.[15]

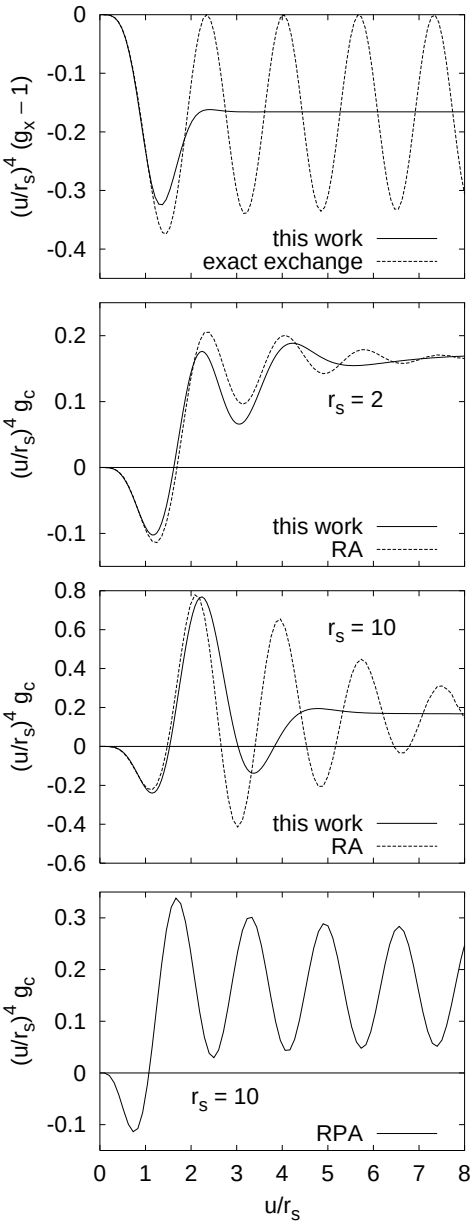


FIG. 4: Upper panel: long-range part of the exchange hole. Our nonsoscillatory model is compared with the exact exchange. Second and third panel: long-range part of the correlation hole. Our nonoscillatory model is compared with g_c obtained from the Richardson and Ashcroft[18] (RA) local-field factor. In the lowest panel the random-phase-approximation (RPA) result for $r_s = 10$ is also shown. All curves are for the $\zeta = 0$ gas.

C. Sum rules

We want our correlation hole to satisfy the particle-conservation sum rule and the plasmon sum rule, and to recover the "exact" correlation energy. Our new parametrization of the function $\overline{f}_1(v)$ satisfies the particle-conservation sum rule, and recovers the exact

plasmon coefficient and the $\ln r_s$ term of the resulting correlation energy. Thus, we only have to require that the remaining part of our $\overline{g}_c$ gives zero contribution to (i) the particle-conservation sum rule and (ii) the plasmon sum rule, and (iii) recovers the correlation energy beyond the $\ln r_s$ term. In this way we have three linear equations for the three parameters c_4, c_5 and c_6:

$$\sum_{n=1}^{6} \tilde{c}_n \int_0^\infty e^{-t^2} t^{n+1} dt = A\, S(\alpha) \tag{33}$$

$$\sum_{n=1}^{6} \tilde{c}_n \int_0^\infty e^{-t^2} t^{n+3} dt = A\, P(\alpha) \tag{34}$$

$$\sum_{n=1}^{6} \tilde{c}_n \int_0^\infty e^{-t^2} t^{n} dt = -A\, R(\alpha) + E, \tag{35}$$

where $\tilde{c}_n = c_n/d^{\frac{n-1}{2}}$, $t = \sqrt{d} k_F u/\phi$, $A = \phi r_s d/\kappa$, $\alpha = \phi^2 \kappa (r_s/d)^{1/2}$, and

$$S(\alpha) = \int_0^\infty \overline{f}_1(\alpha t) e^{-t^2} \left(1 + t^2 + \tfrac{1}{2} t^4\right) dt \tag{36}$$

$$P(\alpha) = \int_0^\infty \overline{f}_1(\alpha t) e^{-t^2} t^2 \left(1 + t^2 + \tfrac{1}{2} t^4\right) dt \tag{37}$$

$$R(\alpha) = \int_0^\infty \frac{\overline{f}_1(\alpha t)}{t} \left[1 - e^{-t^2} \left(1 + t^2 + \tfrac{1}{2} t^4\right)\right] dt \tag{38}$$

$$E = \frac{2 r_s d}{3\,\phi^2} \left(\frac{9\pi}{4}\right)^{2/3} \epsilon_c(r_s, \zeta). \tag{39}$$

The functions $S(\alpha)$, $P(\alpha)$ and $R(\alpha)$ can be obtained analytically and are reported in Appendix C. The parameters c_4, c_5 and c_6 are then equal to

$$\begin{aligned}
\tilde{c}_4 &= \{100\sqrt{\pi}(3\pi - 8)\tilde{c}_1 + (690\pi - 2048)\tilde{c}_2 + \sqrt{\pi}(225\pi \\
&\quad -672)\tilde{c}_3 + (8192 - 2100\pi) A S(\alpha) + A P(\alpha)(600\pi - \\
&\quad 2048) + 960\sqrt{\pi}[A R(\alpha) - E]\}/[4(512 - 165\pi)] \quad (40) \\
\tilde{c}_5 &= 2\{(30\pi - 128)\tilde{c}_1 - 8\sqrt{\pi}\tilde{c}_2 + (39\pi - 128)\tilde{c}_3 - \\
&\quad 144\sqrt{\pi} A S(\alpha) + 16\sqrt{\pi} A P(\alpha) - 256[A R(\alpha) \\
&\quad -E]\}/(512 - 165\pi) \quad (41) \\
\tilde{c}_6 &= \{\sqrt{\pi}(180\pi - 624)\tilde{c}_1 + (150\pi - 512)\tilde{c}_2 + \sqrt{\pi}(135\pi \\
&\quad -432)\tilde{c}_3 + (3072 - 1260\pi) A S(\alpha) + A P(\alpha)(360\pi - \\
&\quad 1024) - 480\sqrt{\pi}[A R(\alpha) - E]\}/[6(165\pi - 512)]. \quad (42)
\end{aligned}$$

D. Positivity constraint in the low-density limit

The nonlinear parameter d can be fixed by imposing the condition that $\overline{g}_{xc}$ remains positive when $r_s \to \infty$. The short-range behavior imposed on our $\overline{g}_c$ ensures that the small-u expansion of the corresponding $\overline{g}_{xc}$ has coefficients which are always ≥ 0 through order u^2, and which become zero in the low-density or strongly-correlated limit. We have checked that, if we want to have a positive $\overline{g}_{xc}$ for all densities, we only need to require that also the u^3 coefficient (equal to $c_4 - d\, c_2$) becomes 0 when $r_s \to \infty$, according to the cusp condition for parallel-spin pairs.[12,15,21] We thus have an equation for $d(\zeta)$:

$$\lim_{r_s \to \infty} c_4(r_s, \zeta) - d(\zeta) c_2(r_s, \zeta) = 0. \tag{43}$$

Equation (43) is rather complicated since c_4 also depends nonlinearly on d. However, it can be solved numerically for each ζ, and, when the Perdew-Wang[33] parametrization of the correlation energy is used in Eq. (39), the result is very well fitted by

$$d(\zeta) = d(0) \left[(1+\zeta)^{2/3} + (1-\zeta)^{2/3} - 1\right], \tag{44}$$

with $d(0) = 0.131707$.

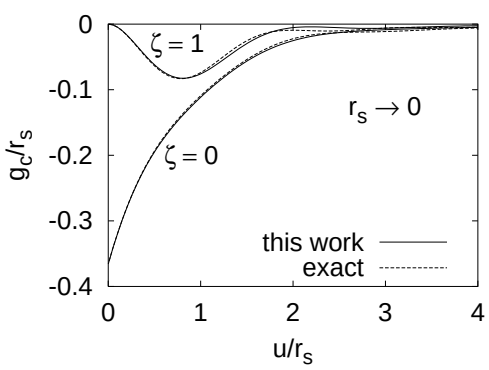


FIG. 5: Coulomb correlation contribution to the pair-distribution function for the uniform electron gas for the paramagnetic ($\zeta = 0$) and ferromagnetic ($\zeta = 1$) state in the high density ($r_s \to 0$) limit. The result from our analytic model is compared with the exact calculation of Refs. 13,19.

V. RESULTS FOR THE EXCHANGE-CORRELATION HOLE

In the next three subsections we present and discuss our results for the nonoscillatory g_x, g_c and g_{xc} in the whole ($0 < r_s < \infty$) density range. We have used the correlation energy ϵ_c as parametrized by Perdew and Wang,[33] which was built with the Quantum Monte Carlo data of Ref. 3 as an input. It is however straightforward to build into our equations an *ab initio* ϵ_c for the 3D uniform gas when available,[34] showing that the exact constraints suffice to determine g_{xc} without the need for any "numerical experiment".

A. Metallic densities

In the six upper panels of Fig. 3 we compare our analytic g_c with the Quantum Monte Carlo (QMC) data of Ceperley and Alder[3] (CA) and of Ortiz, Harris and Ballone[17] (OHB) for $r_s = 2$, 5 and 10, and for $\zeta = 0$ (left) and $\zeta = 1$ (right). In the $\zeta = 0$ case, we also report

g_c as obtained by the dynamic local-field-factor model of Richardson and Ashcroft[18] (RA) via the fluctuation-dissipation theorem (as in Ref. 35). The RA model yields very accurate correlation energies $\epsilon_c(r_s, \zeta = 0)$,[35] and we find that the RA g_c is in very good agreement with QMC data except at small u. The limit $u \to 0$ is not correctly included in the RA parametrization of the local-field factor, which violates the Pauli principle in real space.

We see that our model is in fair agreement with QMC data for the paramagnetic gas. In the ferromagnetic case, where the pair-correlation function shows stronger oscillations even at intermediate densities, the agreement is less satisfactory (as in the model of Ref. 2). This is not surprising, since our model does not take into account the energetically unimportant oscillations: it only includes the minimum number of oscillations needed to fulfill the sum rules. This is evident in the second and third panel of Fig. 4, where g_c is multiplied by $(u/r_s)^4$. In this way, the long-range oscillations are amplified and become clearly visible even at metallic densities: we can thus compare our model (solid line) with the RA result (dashed line). This is done at $r_s = 2$ and 10. The many exact properties imposed on the RA local-field factor and the first three left panels of Fig. 3 suggest that the long-range part of the RA g_c is very reliable and that the oscillations are probably accurately described. One clearly sees in Fig. 4 how our model follows the first oscillation and averages out the others. In the lowest panel of Fig. 4, the long-range oscillations of the random-phase approximation (RPA) g_c at $r_s = 10$ are also shown. At large r_s, the RPA oscillations of g_c tend to cancel the ones of g_x (first panel), while the effect of a dynamic local-field factor clearly inverts this tendency: the oscillations of the RA g_c (second and third panel) are almost in phase with the oscillations of g_x. We interpret this to mean that the RA g_{xc} of the low-density uniform electron gas is building up an incipient Wigner-crystal-like order of the other electrons around a given electron.

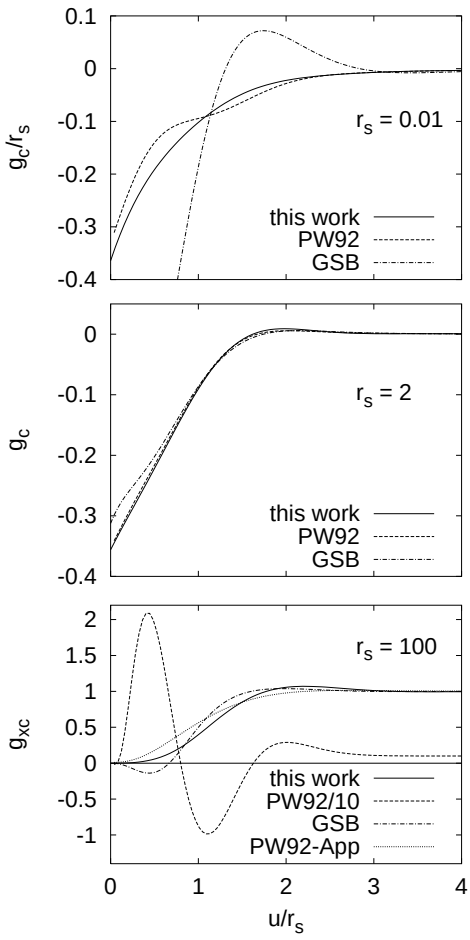


FIG. 6: Comparison of the present work with the models of Ref. 2 (PW92) and of Ref. 12 (GSB) at high densities (first panel), metallic densities (second panel) and in the low-density regime (third panel). In the $r_s = 100$ case the original PW92 curve has been divided by 10, and the low-density form proposed in the Appendix of Ref. 2 (PW92-App) is also reported. All curves are for the paramagnetic ($\zeta = 0$) gas.

B. High density

In the high-density limit, $g_c = 2\overline{g}_c$ goes to zero, so that $g_{xc} \to g_x$. It has been shown[2,13,19] that in the $r_s \to 0$ limit g_c/r_s remains finite and goes to a well defined function of u/r_s, which has been computed exactly.[13,19] In Fig. 5 we compare this exact calculation (dashed line) with our model (solid line), computed at $r_s = 10^{-5}$, for $\zeta = 0$ and $\zeta = 1$. We see that (i) our model does not break down as $r_s \to 0$, and (ii) there is fair agreement with the exact result. Previous models[2,12] for g_c usually break down at $r_s \sim 0.1$. Feature (i) is due to the new parametrization of $\overline{f}_1(v)$ which exactly fulfills the particle-conservation sum rule, while feature (ii) is due to the short-range behavior taken from Ref. 15, which includes the exact high-density limit of the short-range coefficients.

C. Low density

In the low-density or strongly-correlated limit, we expect that g_{xc} (equal to $\overline{g}_{xc}$ in this case) does not depend on ζ, since in this limit the Pauli principle in real space becomes irrelevant with respect to the Coulomb repulsion. In the lower panel of Fig. 1 we report our model at $r_s = 10^5$ for three different values of the spin polarization ζ. We see that the ζ dependence of our low-density g_{xc} is indeed very weak, and that, unlike previous parametrizations,[2,12] our model never gives rise to an unphysical negative pair-distribution function. Figure 1 also offers a view on the same scale of the extreme high-density limit of g_{xc} (equal to the exchange-only pair-distribution function, first panel) and of the extreme low-

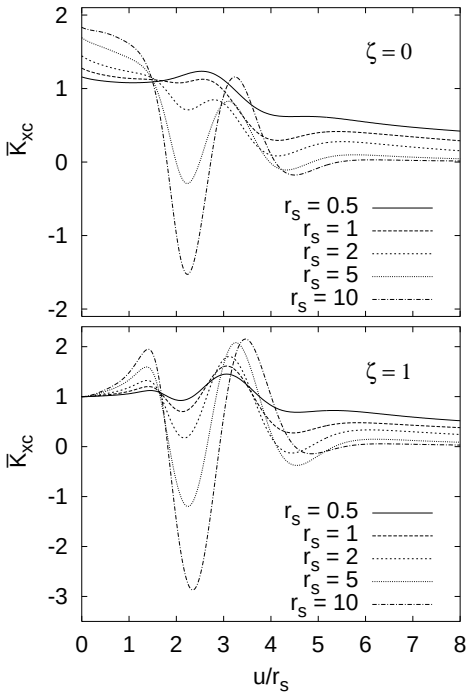


FIG. 7: The correlation factor $\overline{K}_{xc}$ defined in Eq. (45) for the paramagnetic (upper panel) and ferromagnetic (lower panel) uniform electron gas.

density limit (second panel). We see how the ζ dependence of g_{xc}, which is very strong in the $r_s \to 0$ limit, is cancelled by correlation in the $r_s \to \infty$ limit. The low-density limit of our $g_c = g_{xc} - g_x$ is reported in the two lowest panels of Fig. 3 for $\zeta = 0$ or $\zeta = 1$.

D. Comparison with previous analytic models

In Fig. 6 the present model is compared with the parametrizations of Perdew and Wang[2] (PW92) and of Gori-Giorgi, Sacchetti and Bachelet[12] (GSB). In the first panel, we see that in the high-density regime ($r_s = 0.01$) the PW92 model starts to break down,[14,19] and that the GSB parametrization is completely unable to describe such high densities. (This is due to the wrong $r_s \to 0$ behavior of the GSB on-top pair density.) At $r_s = 2$, well inside the metallic regime, we see (second panel) that the present work is very close to the PW92 model and slightly deviates from the GSB curve at $u/r_s \lesssim 1$. Finally, in the third panel we show the total pair-distribution function g_{xc} at $r_s = 100$: the PW92 model in its original form completely blows up, while the GSB model becomes negative at $u/r_s \lesssim 1$ but is still "reasonable". The low-density form proposed in the Appendix of Ref. 2 (PW92-App) is also reported: it corresponds to an exchange-correlation hole narrower than the present one.

E. Features of the "correlation factor"

To better see the effects of correlation, we define a "correlation factor"

$$\overline{K}_{xc}(r_s, \zeta, k_F u) = \frac{\overline{g}_{xc} - 1}{g_x - 1} = 1 + \frac{\overline{g}_c}{g_x - 1} \qquad (45)$$

which morphs the exchange hole into the exchange-correlation hole, and is displayed in Fig. 7. We must of course use non-oscillatory models here, since the exact $g_x - 1$ has nodes which would create singularities in Eq. (45). Figure 7 shows that $\overline{K}_{xc} \to K_x = 1$ in the $r_s \to 0$ limit. For typical valence-electron densities, we see that correlation enhances or deepens the hole ($\overline{K}_{xc} > 1$) around an electron for $u/r_s \lesssim 1.5$, while it screens out the long-range part of the hole. Because of the exact cancellation of the u^{-4} and u^{-6} long-range terms between $\overline{g}_c$ and $g_x - 1$, $\overline{K}_{xc}$ at large u goes to 0 like u^{-4}. For $r_s > 2$, $\overline{K}_{xc}$ can be negative in the range $1.5 \lesssim u/r_s \lesssim 3$, corresponding to a positive peak in $\overline{g}_{xc} - 1$. We can think of $\overline{K}_{xc}(r_s, \zeta, k_F u)/u$ as an effective, density-dependent screened electron-electron interaction whose exchange energy equals the exchange-correlation energy of the Coulomb interaction $1/u$.

The correlation factor has a possible application[30,31] to the modelling of exchange and correlation in systems of non-uniform density. First we note that the exchange-correlation energy is fully determined by the spherical average $n_{xc}(\mathbf{r}, u)$ of the hole,[1]

$$n_{xc}(\mathbf{r}, u) = \int \frac{d\Omega_{\mathbf{u}}}{4\pi} n_{xc}(\mathbf{r}, \mathbf{r} + \mathbf{u}). \qquad (46)$$

A possible "correlation factor model"[31] for $n_{xc}(\mathbf{r}, u)$ is

$$n_{xc}(\mathbf{r}, u) = \overline{K}_{xc}(\mathbf{r}, u)\, n_x(\mathbf{r}, u), \qquad (47)$$

where $n_x(\mathbf{r}, u)$ is the exact exchange hole. $\overline{K}_{xc}$ for a non-uniform density could be constructed from Eq. (45) by inserting into Eq. (22) (or a simplification thereof) an $\mathbf{r}$-dependent set of linear parameters c_n chosen to satisfy exact constraints on n_{xc}. The result would presumably be a model for exact exchange and approximate correlation compatible therewith. The screening of the long-range part of the exact exchange hole is essential for a proper description of molecules.[32]

VI. SPIN RESOLUTION

We can define spin-resolved pair-distribution functions which describe spatial correlations between $\uparrow\uparrow$, $\downarrow\downarrow$, and $\uparrow\downarrow$ electron pairs. Their normalization is such that the spin-averaged g_{xc} of Eq. (1) is equal to

$$g_{xc} = \left(\frac{1+\zeta}{2}\right)^2 g_{xc}^{\uparrow\uparrow} + \left(\frac{1-\zeta}{2}\right)^2 g_{xc}^{\downarrow\downarrow} + \left(\frac{1-\zeta^2}{2}\right) g_{xc}^{\uparrow\downarrow}. \qquad (48)$$

While the spin resolution of the exchange-only pair-distribution function g_x is well known,[2] the correlation part is much more delicate, and an accurate analytic representation is only available[12] for $\zeta = 0$ in the density range $0.8 \leq r_s \leq 10$.

The model presented in Sec. IV can be used to build up spin-resolved correlation functions provided that the spin resolution of the input quantities is known. The input quantities are (i) the RPA long-range part, (ii) the short-range coefficients from the solution of the Overhauser model, and (iii) the correlation energy. Once these input quantities are known, in fact, one can build, say, $\overline{g}_c^{\uparrow\downarrow}$, starting from the same Eq. (22), using the RPA $\uparrow\downarrow$ long-range part, and putting the $\uparrow\downarrow$ short-range coefficients into Eqs. (30)-(32), and $\epsilon_c^{\uparrow\downarrow}$ into Eq. (39). Finally, the positivity constraint of $g_{xc}^{\uparrow\downarrow}$ in the low-density limit can be applied to find $d_{\uparrow\downarrow}(\zeta)$, as done in Sec. IV D.

The first point is thus to see whether the quantities (i)-(iii) are available in their spin-resolved contributions. The RPA long-range part is easily spin-resolved for the $\zeta = 0$ gas,[12,14] while its spin resolution in the partially polarized gas is less trivial. The short-range coefficients from the Overhauser model are available as $\uparrow\uparrow$, $\downarrow\downarrow$ and $\uparrow\downarrow$ separate contributions.[15] The correlation energy represents the major problem: at $\zeta = 0$ it can be easily spin resolved in the high- and low- density limits, while at intermediate densities the best estimate is probably the one given in Ref. 12. Almost nothing about the spin resolution of ϵ_c is known for the $\zeta \neq 0$ gas, except in the extreme low-density limit, when the system becomes ζ-independent.

Here, we show results for $g_c^{\uparrow\downarrow}$ in three cases: the extreme low-density limit, the high-density limit of the paramagnetic gas, and the $r_s = 2$, $\zeta = 0$ case. The low-density limit must be treated first, since it is necessary to determine $d_{\uparrow\downarrow}(\zeta)$ through the positivity constraint on $g_{xc}^{\uparrow\downarrow}$ when $r_s \to \infty$.

When $\zeta = 0$, the spin-resolution within RPA is very simple: up-up and up-down interactions contribute the same amount to correlation.[12,14] The long-range part of our $\overline{g}_c^{\uparrow\downarrow}$ can thus be built using the function $\overline{f}_1(v)$ of Eq. (28) with the same parameters of Appendix B. While the spin-averaged nonoscillatory long-range behavior computed within RPA is also exact beyond it at all densities, its spin resolution is exact beyond RPA only when $r_s \to 0$.[36] We keep on using it even in the extreme low-density limit, since it is the only way to build up a spin-resolved g_c starting from our model. As we shall see, the results obtained are reasonable, and justify our choice. When $r_s \to \infty$, we expect the statistics to be energetically unimportant,[37] so that $\epsilon_{xc}^{\uparrow\uparrow} = \epsilon_{xc}^{\downarrow\downarrow} = \epsilon_{xc}^{\uparrow\downarrow} = \epsilon_{xc}$. We thus find $\epsilon_c^{\uparrow\downarrow} = \epsilon_{xc} = -0.892/r_s$, where the numerical coefficient corresponds to the Perdew-Wang parametrization[33] of ϵ_c. The positivity constraint on $g_{xc}^{\uparrow\downarrow}$ gives

$$d_{\uparrow\downarrow}(\zeta) = d_{\uparrow\downarrow}(0)\left[(1+\zeta)^{2/3} + (1-\zeta)^{2/3} - 1\right], \qquad (49)$$

with $d_{\uparrow\downarrow}(0) = 0.0885717$. The results for $g_{xc}^{\uparrow\downarrow}$ are shown in Fig. 8, at $r_s = 10^5$, for $\zeta = 0$ and $\zeta = 1$.

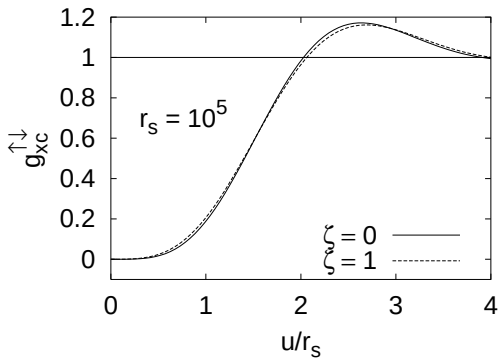


FIG. 8: Up-down pair-distribution function for the uniform electron gas in the low-density limit.

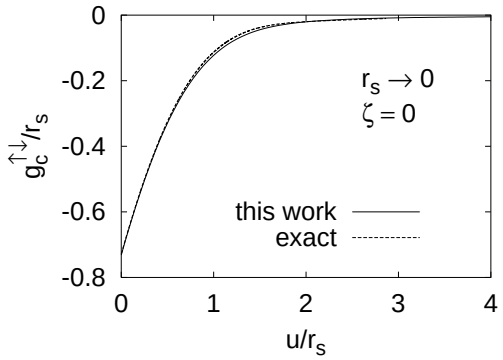


FIG. 9: Up-down Coulomb correlation contribution to the pair-distribution function for the paramagnetic ($\zeta = 0$) uniform electron gas in the high density ($r_s \to 0$) limit. The result from our analytic model is compared with the exact calculation of Ref. 19.

For the high-density limit of the paramagnetic gas, all the spin-resolved input quantities are exactly known. It is thus the best case to test our model. When $r_s \to 0$, the spin-resolution from RPA is exact also beyond it: the long-range part of $\overline{g}_c^{\uparrow\downarrow}$ is in this case *exactly* described by Eq. (28) with the parameters of Appendix B. The correlation energy, in this limit,[12,26] is simply equal to the spin-averaged correlation energy of Eq. (27) with ζ set to zero. The short-range $\uparrow\downarrow$ coefficients from Ref. 15 include the exact spin-resolved high-density limit of the $\zeta = 0$ gas. The so-obtained $g_c^{\uparrow\downarrow}$ is shown in Fig. 9, together with the exact calculation from Ref. 19, which is, in this case, equal to the RPA result. We find very good agreement.

At metallic densities, we used the spin-resolved ϵ_c for the $\zeta = 0$ gas from Ref. 12, and the RPA spin resolution for the long-range part. In Fig. 10, we report our results for $g_c^{\uparrow\downarrow}$ and $g_c^{\uparrow\uparrow} = 2g_c - g_c^{\uparrow\downarrow}$ at $r_s = 2$, together with the QMC data of Ref. 17, and with the values that we have obtained from the Richardson and Ashcroft (RA) local-field factors.[18] We see that our result is reasonable, but does not accurately agree with the QMC data. In this

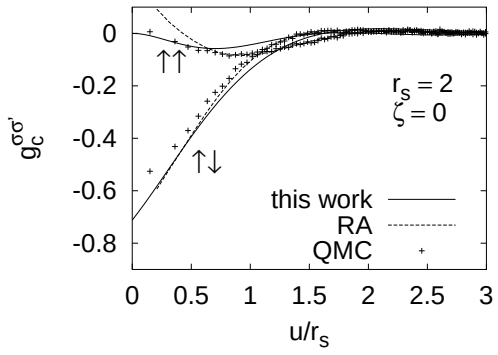


FIG. 10: Spin-resolved Coulomb correlation contribution to the pair-distribution functions for the paramagnetic uniform electron gas at density $r_s = 2$. The present model is compared with the Quantum Monte Carlo (QMC) data from Ref. 17 and with the result obtained from the local-field factors of Richardson and Ashcroft[18] (RA).

respect, the RA results are much better for $u/r_s \gtrsim 0.7$, while they blow up in the short-range part, since they do not satisfy the Pauli principle in real space. As said, the spin resolution is very delicate, so that an analytic model is very difficult to build up. The best analytic representation of $g_c^{\uparrow\downarrow}$ and $g_c^{\uparrow\uparrow}$ at metallic densities is probably the one of Ref. 12, which was built to interpolate the QMC data of Ref. 17 accurately.

VII. WAVEVECTOR ANALYSIS OF THE KINETIC ENERGY OF CORRELATION

Wavevector analysis[20] is usually a study of the static structure factor of Eq. (6). The wavevector analyses of the correlation energy ϵ_c and of the potential energy of correlation v_c have often been reported,[12,35,38] while the kinetic energy of correlation t_c is much less studied. We can decompose $t_c(r_s,\zeta)$ into contributions from different wavevectors of a density fluctuation,

$$t_c(r_s,\zeta) = \tfrac{3}{2}\int_0^\infty dq\, q^2\, \mathcal{T}_c(r_s,\zeta,q), \tag{50}$$

where $q = k/k_F$. Since $t_c = \epsilon_c - v_c$, the wavevector analysis of t_c is just the difference between those for ϵ_c and v_c:

$$\mathcal{T}_c(r_s,\zeta,q) = \frac{2k_F}{3\pi}\frac{[\overline{S}_c(r_s,\zeta,q) - S_c(r_s,\zeta,q)]}{q^2}. \tag{51}$$

The small-q limit of $\mathcal{T}_c$ can be obtained by the plasmon sum rule,

$$\mathcal{T}_c(r_s,\zeta,q\to 0) = \tfrac{\sqrt{3}}{4}\, r_s^{-3/2} + O(q^2), \tag{52}$$

and its leading term is independent of ζ, as expected from Eq. (14). To write down the large-q limit of $\mathcal{T}_c$ we need to expand $\overline{S}_c$ and S_c for large arguments. We know that[12,21,26,39]

$$S_c(r_s,\zeta,q\to\infty) = -\frac{4}{3\pi k_F}\frac{2g_{xc}(r_s,\zeta,u=0)}{q^4} + O(q^{-6}), \tag{53}$$

from which we can also obtain the large-q limit of $\overline{S}_c$,

$$\overline{S}_c(r_s,\zeta,q\to\infty) = \frac{\overline{\gamma}}{q^4} + O(q^{-6}), \tag{54}$$

where

$$\overline{\gamma} = -\frac{8}{3\pi}\left(\frac{4}{9\pi}\right)^{1/3}\frac{1}{r_s}\int_0^{r_s} r_s'\, g_{xc}(r_s',\zeta,u=0)\, dr_s'. \tag{55}$$

Through the cusp condition of Eq. (13), we see that the large-q limit of $\overline{S}_c$ is determined by the coefficient of u/r_s in the small-u expansion of $\overline{g}_c$, $\overline{a}_1(r_s,\zeta)$ [see Eqs. (35) and (37) of Ref. 15], related to $c_2(r_s,\zeta)$ of Eq. (31) by $\overline{a}_1 = (9\pi/4)^{1/3}c_2/\phi$. We thus have

$$\mathcal{T}_c(r_s,\zeta,q\to\infty) = \frac{8}{9\pi^2}\frac{\left[2g_{xc}(r_s,\zeta,u=0) - 2\frac{\overline{a}_1(r_s,\zeta)}{r_s}\right]}{q^6}. \tag{56}$$

In Fig. 11, we report $\mathcal{T}_c$ for the $\zeta = 0$ gas, for two different densities, $r_s = 2$ and $r_s = 5$. We clearly see that the small wavevector contribution to t_c comes from the kinetic energy of the long-wavelength zero-point plasmons, and that the decay of the plasmon contribution with increasing wavevector k is gradual. The corresponding result from the Richardson and Ashcroft local field factor[18] is also shown. The Richardon-Ashcroft model gives a good description of plasmon dispersion and damping.[40]

It is also interesting to compare $\mathcal{T}_c$ with the decomposition of the kinetic energy of correlation into contributions from different wavevectors of a quasi-electron. For $\zeta = 0$, we can write

$$t_c(r_s,\zeta=0) = \tfrac{3}{2}\int_0^\infty dq\, q^2\, n_c(r_s,\zeta=0,q)\,(k_F\, q)^2. \tag{57}$$

Here n_c is the correlation contribution to the momentum distribution, $n_c(q) = n(q) - n_0(q)$, and n_0 is the Fermi step function. The leading term in the small-q expansion of $k_F^2 q^2 n_c$ is proportional to q^2, and is thus rather different from the corresponding behavior of $\mathcal{T}_c$, Eq. (52). On the other hand, in the large-q limit we have[39]

$$k_F^2 q^2 n_c(r_s,\zeta=0,q\to\infty) = \frac{8}{9\pi^2}\frac{g_{xc}(r_s,\zeta=0,u=0)}{q^6}, \tag{58}$$

a behavior very similar to Eq. (56). This is not surprising, since the large-q limits of both S_c and n_c are determined by the downward-pointing kinks in the many body wavefunction [producing the cusp of Eq. (13)] which occur whenever two electrons of antiparallel spin come together. In the $r_s \to 0$ limit, Eqs. (56) and (58) become equal. A study of the equations linking S_c and n_c from the point of view of density matrix functional theory is reported in Ref. 41.

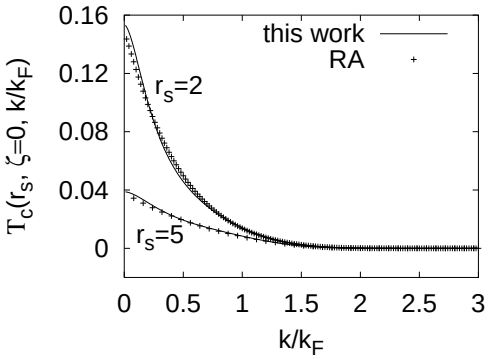


FIG. 11: Wavevector analysis of the kinetic energy of correlation at $r_s = 2$ and $r_s = 5$ for the paramagnetic gas. The function $\mathcal{T}_c(r_s, \zeta, k)$ is defined in Eq. (51). The present work is compared with the result obtained from the Richardson and Ashcroft[18] (RA) local-field factor.

VIII. CONCLUSIONS AND FUTURE DIRECTIONS

The known exact constraints summarized in Sec. II, plus the random phase approximation for long-range ($u \to \infty$) correlation, the extended Overhauser model[15] for short-range ($u \to 0$) correlation, and the correlation energy $\epsilon_c(r_s, \zeta)$, suffice to determine the pair distribution function $g_{xc}(r_s, \zeta, k_F u)$ of a uniform electron gas over the whole density range, including the high-density ($r_s \to 0$) and low-density ($r_s \to \infty$) limits, apart from energetically-unimportant long-range oscillations. The analytic formulas we have so constructed for the coupling-constant-averaged $\overline{g}_{xc}$ should be useful for further developments and applications of density-functional approximations for the exchange-correlation energy of a non-uniform density.

For metallic densities ($2 < r_s < 10$) with $\zeta = 0$ or 1, our g_{xc} is in good agreement with Quantum Monte Carlo.[3,17] In the same density range for $\zeta = 0$, it also agrees with the g_{xc} we have calculated from the Richardson-Ashcroft[18] dynamic local-field factor, except near $u = 0$ where the Richardson-Ashcroft model was found to break down (although this model seems to describe the long-range oscillations correctly). In the $r_s \to 0$ limit for small $k_F u$, our g_{xc} agrees with the results of perturbation theory to zero-th (exchange) or first order[13,19] in the electron-electron interaction. The static structure factor S_{xc} is also modelled accurately, neglecting the non-analytic structure of the exact S_{xc} at $k = 2k_F$ arising from long-range oscillations.[41]

Our formulas can also be used to spin-resolve g_{xc} into $\uparrow\uparrow$, $\downarrow\downarrow$, and $\uparrow\downarrow$ components (Sec. VI), when the spin resolution of ϵ_c is known (as it is in the high- and low-density limits). The additional information in the spin resolution might well be used to construct more accurate density functionals for the correlation energy.

We have also examined two physically-different wavevector analyses of the kinetic energy of correlation in the uniform electron gas, finding them the same only in the limits of large wavevector and high density. We have also found that the decay of the plasmon contribution with increasing wavevector k is gradual.

In the future, it may be possible to construct the correlation energy $\epsilon_c(r_s, \zeta)$ and its spin resolution $\epsilon_c^{\sigma\sigma'}(r_s, \zeta)$ directly by interpolation between known limits,[34] without using *any* Monte Carlo or other data. This development would probably not give us a better $\epsilon_c(r_s, \zeta)$ than we already have, but would provide the first spin resolution over the whole range of r_s and ζ; it would also show that the known exact constraints are by themselves sufficient to determine g_{xc}. The extended Overhauser model[15] might be evaluated for ζ different from zero, to test and refine the spin-scaling relations used in Ref. 15. The extended Overhauser model can also be made more selfconsistent.[42]

A small `FORTRAN77` subroutine which numerically evaluates our $\overline{g}_c$ [Eq. (22)] can be downloaded at `http://axtnt2.phys.uniroma1.it/PGG/elegas.html`.

Acknowledgments

This work was supported by the Fondazione Angelo Della Riccia (Firenze, Italy), the MURST (the Italian Ministry for University, Research and Technology) through COFIN99, and by the U.S. National Science Foundation under grants DMR-9810620 and DMR-0135678.

APPENDIX A: NONOSCILLATORY EXCHANGE HOLE IN RECIPROCAL SPACE

In reciprocal space, the exchange-only static structure factor is equal to

$$S_x(\zeta, k/k_F) = 1 + \frac{2}{3\pi}\left[(1+\zeta)\tilde{J}\left(\frac{k}{k_F(1+\zeta)^{1/3}}\right) + (1-\zeta)\tilde{J}\left(\frac{k}{k_F(1-\zeta)^{1/3}}\right)\right], \quad \text{(A1)}$$

where $\tilde{J}(k)$ is defined by Eq. (19). From our parametrization of $\langle J(y)\rangle$ [Eq. (18)] we obtain

$$\tilde{J}(k) = \frac{9\pi}{16}k\left[1 - \mathrm{erf}\left(\frac{k}{2\sqrt{A_x}}\right)\right] - \frac{3\sqrt{\pi}}{32}e^{-\frac{k^2}{4A_x}} \times \left(9\sqrt{A_x} + \frac{k^2 - 6A_x}{4\sqrt{A_x}}\right) + \frac{\sqrt{\pi}}{4}e^{-\frac{k^2}{4D_x}}\left[\frac{B_x}{D_x^{3/2}} + \frac{C_x(6D_x - k^2)}{4D_x^{7/2}} + \frac{E_x(60D_x^2 - 20D_x k^2 + k^4)}{16D_x^{11/2}} + \frac{F_x(840D_x^3 - 420D_x^2 k^2 + 42D_x k^4 - k^6)}{64D_x^{15/2}}\right]. \quad \text{(A2)}$$

APPENDIX B: LONG-RANGE CORRELATION HOLE IN RECIPROCAL SPACE

The function $f(z,0)$ corresponding to our Eq. (28) is

$$\begin{aligned} f(z,0) &= \frac{1}{2zb^8}\Big\{a_0 - \frac{e^{-bz}}{48}\big[48a_0 + (33a_0b - 3a_1b^3 \\ &\quad -3a_2b^5 - 15a_3b^7)z + (9a_0b^2 - 3a_1b^4 - \\ &\quad 3a_2b^6 + 9a_3b^8)z^2 + (a_0b^3 - a_1b^5 + a_2b^7 \\ &\quad -a_3b^9)z^3\big]\Big\} - \frac{b_2}{6\pi\, z}\frac{\partial^3 \mathcal{I}(b,z)}{\partial (b^2)^3}, \end{aligned} \tag{B1}$$

where

$$\mathcal{I}(b,z) = \frac{1}{2b}\left[e^{bz}E_1(bz) - e^{-bz}E_1(-bz)\right], \tag{B2}$$

and, with $x > 0$,

$$\begin{aligned} E_1(x) &= \int_x^\infty \frac{e^{-t}}{t}dt \\ E_1(-x) &= -\mathrm{Ei}(x) = -\mathrm{PV}\left(\int_{-\infty}^{x}\frac{e^t}{t}dt\right). \end{aligned}$$

Here PV means the Cauchy principal value integral.[43]

The parameter values which satisfy Eqs. (25) and (26), give rise to a zero coefficient for the z^3 term in the small-z expansion of $f(z,0)$, and accurately fit our RPA data,[16] are

$$\begin{aligned} a_0 &= 2b^8C_0 \\ a_1 &= \frac{6b^3}{\pi^2}\left[\pi^2C_0b^3 + 78b - 256\sqrt{3}\right] \\ a_2 &= 48b^2/\pi^2 \\ a_3 &= 12/\pi^2 \\ b_2 &= \frac{3b^4}{\pi}\left[96\sqrt{3} - 36b - b^3C_0\pi^2\right] \\ C_0 &= -2(1-\ln 2)/\pi^2 \\ b &= 7.8. \end{aligned}$$

APPENDIX C: ANALYTIC EXPRESSIONS FOR THE FUNCTIONS $S(\alpha)$, $P(\alpha)$ AND $R(\alpha)$

The three functions of Eqs. (36), (37) and (38), which enter our model for $\overline{g}_c$, are given by a linear combination of integrals of the kind

$$\mathcal{I}_m^n(\alpha) = \int_0^\infty \frac{x^n e^{-x^2}}{[(\alpha x)^2 + b^2]^m}dx \tag{C1}$$

$$\mathcal{I}_m^{-1}(\alpha) = \int_0^\infty \frac{1 - e^{-x^2}}{x[(\alpha x)^2 + b^2]^m}dx. \tag{C2}$$

We obtain for $S(\alpha)$, $P(\alpha)$ and $R(\alpha)$:

$$\begin{aligned} S(\alpha) &= a_0\mathcal{I}_4^0(\alpha) + (a_0 + a_1\alpha^2)\mathcal{I}_4^2(\alpha) + (\tfrac{1}{2}a_0 + a_1\alpha^2 + \\ &\quad a_2\alpha^4)\mathcal{I}_4^4(\alpha) + (\tfrac{1}{2}a_1\alpha^2 + a_2\alpha^4 + a_3\alpha^6)\mathcal{I}_4^6(\alpha) + \\ &\quad (\tfrac{1}{2}a_2\alpha^4 + a_3\alpha^6)\mathcal{I}_4^8(\alpha) + \tfrac{1}{2}a_3\alpha^6\mathcal{I}_4^{10}(\alpha) + b_2\alpha \times \\ &\quad \left[\mathcal{I}_4^1(\alpha) + \mathcal{I}_4^3(\alpha) + \tfrac{1}{2}\mathcal{I}_4^5(\alpha)\right] \end{aligned} \tag{C3}$$

$$\begin{aligned} P(\alpha) &= a_0\mathcal{I}_4^2(\alpha) + (a_0 + a_1\alpha^2)\mathcal{I}_4^4(\alpha) + (\tfrac{1}{2}a_0 + a_1\alpha^2 + \\ &\quad a_2\alpha^4)\mathcal{I}_4^6(\alpha) + (\tfrac{1}{2}a_1\alpha^2 + a_2\alpha^4 + a_3\alpha^6)\mathcal{I}_4^8(\alpha) + \\ &\quad (\tfrac{1}{2}a_2\alpha^4 + a_3\alpha^6)\mathcal{I}_4^{10}(\alpha) + \tfrac{1}{2}a_3\alpha^6\mathcal{I}_4^{12}(\alpha) + b_2\alpha \times \\ &\quad \left[\mathcal{I}_4^3(\alpha) + \mathcal{I}_4^5(\alpha) + \tfrac{1}{2}\mathcal{I}_4^7(\alpha)\right] \end{aligned} \tag{C4}$$

$$\begin{aligned} R(\alpha) &= a_0\mathcal{I}_4^{-1}(\alpha) - (a_0 + a_1\alpha^2)\mathcal{I}_4^1(\alpha) - (\tfrac{1}{2}a_0 + a_1\alpha^2 + \\ &\quad a_2\alpha^4)\mathcal{I}_4^3(\alpha) - (\tfrac{1}{2}a_1\alpha^2 + a_2\alpha^4 + a_3\alpha^6)\mathcal{I}_4^5(\alpha) - \\ &\quad (\tfrac{1}{2}a_2\alpha^4 + a_3\alpha^6)\mathcal{I}_4^7(\alpha) - \tfrac{1}{2}a_3\alpha^6\mathcal{I}_4^9(\alpha) - b_2\alpha \times \\ &\quad \left[\mathcal{I}_4^0(\alpha) + \mathcal{I}_4^2(\alpha) + \tfrac{1}{2}\mathcal{I}_4^4(\alpha)\right] + \\ &\quad \frac{2a_1 + a_2b^2 + 2a_3b^4}{12b^6} + b_2\frac{5}{32}\frac{\pi}{b^7}, \end{aligned} \tag{C5}$$

where a_0, a_1, a_2, a_3, b_2 and b are given in Appendix B. The integrals of the kind (C1) can be written as

$$\mathcal{I}_m^n(\alpha) = \tilde{\mathcal{I}}_m^n(\alpha/b)/b^{2n}, \tag{C6}$$

$$\tilde{\mathcal{I}}_m^n(r) = \int_0^\infty \frac{x^n e^{-x^2}}{[(rx)^2 + 1]^m}dx, \tag{C7}$$

and starting from

$$\tilde{\mathcal{I}}_1^0(r) = \frac{\pi}{2r^2}e^{1/r^2}\left[1 - \mathrm{erf}\left(\frac{1}{r}\right)\right] \tag{C8}$$

$$\tilde{\mathcal{I}}_1^1(r) = \frac{1}{2r^2}e^{1/r^2}E_1\left(\frac{1}{r^2}\right), \tag{C9}$$

can be computed by differentiation with respect to α and b. The integrals of the kind (C2) can be also obtained by differentiation with respect to b of

$$\mathcal{I}_1^{-1}(\alpha) = \frac{e^{b^2/\alpha^2}E_1(b^2/\alpha^2) + \ln(b^2/\alpha^2) + \gamma}{2b^2}, \tag{C10}$$

where $\gamma = 0.5772156649$.

[1] see, e.g., R.O. Jones and O. Gunnarsson, Rev. Mod. Phys. **61**, 689 (1989).

[2] J. P. Perdew and Y. Wang, Phys. Rev. B **46**, 12947 (1992);

erratum **56**, 7018 (1997).
[3] D. M. Ceperley and B. J. Alder, Phys. Rev. Lett. **45**, 566 (1980).
[4] J. P. Perdew, *Electronic Structure of Solids '91*, edited by P. Ziesche and H. Eschrig (Akademie Verlag, Berlin 1991); J. P. Perdew, K. Burke, and M. Ernzerhof, Phys. Rev. Lett. **77**, 3865 (1996); erratum **78**, 1396 (1997).
[5] J. P. Perdew, K. Burke, and Y. Wang, Phys. Rev. B **54**, 16533 (1996).
[6] O. Gunnarsson, M. Jonson, and B. I. Lundqvist, Phys. Lett. A **59**, 177 (1976); Phys. Rev. B **20**, 3136 (1979).
[7] E. Chacón and P. Tarazona, Phys. Rev. B **37**, 4013 (1988).
[8] P.P. Rushton, D.J. Tozer, and S.J. Clark, Phys. Rev. B **65**, 235203 (2002).
[9] A.D. Becke, J. Chem. Phys. **88**, 1053 (1988).
[10] A.J. Cohen and N.C. Handy, Mol. Phys. **99**, 607 (2001).
[11] P. Ziesche, *Electron Correlations and Material Properties 2*, edited by A. Gonis, N. Kioussis and M. Ciftan (Kluwer Academic/Plenum Publishers, New York 2002), and references therein.
[12] P. Gori-Giorgi, F. Sacchetti, and G.B. Bachelet, Phys. Rev. B **61**, 7353 (2000).
[13] V. A. Rassolov, J. A. Pople, and M. A. Ratner, Phys. Rev. B **59**, 15625 (1999).
[14] K. Schmidt, S. Kurth, J. Tao, and J. P. Perdew, Phys. Rev. B **62**, 2227 (2000).
[15] P. Gori-Giorgi and J. P. Perdew, Phys. Rev. B **64**, 155102 (2001).
[16] Y. Wang and J. P. Perdew, Phys. Rev. B **44**, 13298 (1991).
[17] G. Ortiz, M. Harris, and P. Ballone, Phys. Rev. Lett. **82**, 5317 (1999).
[18] C.F. Richardson and N.W. Ashcroft, Phys. Rev. B **50**, 8170 (1994). See also Ref. 35.
[19] V. A. Rassolov, J. A. Pople, and M. A. Ratner, Phys. Rev. B **62**, 2232 (2000).
[20] D.C. Langreth and J.P. Perdew, Phys. Rev. B **15**, 2884 (1977).
[21] A. K. Rajagopal, J. C. Kimball, and M. Banerjee, Phys. Rev. B **18**, 2339 (1978).
[22] A.W. Overhauser, Can. J. Phys. **73**, 683 (1995).
[23] M.W.C. Dharma-wardana and F. Perrot, Phys. Rev. Lett. **84**, 959 (2000).
[24] P. Nozières and D. Pines, Phys. Rev. **111**, 442 (1958).
[25] D. Pines and P. Nozières, *Theory of Quantum Liquids* (Benjamin, New York, 1966).
[26] P. Gori-Giorgi, F. Sacchetti, and G.B. Bachelet, Physica A **280**, 199 (2000).
[27] N. Iwamoto, Phys. Rev. A **33**, 1940 (1986).
[28] M. Ernzerhof and J.P. Perdew, J. Chem. Phys. **109**, 3315 (1998).
[29] J. Antolin, A. Zarzo, and J.C. Angulo, Phys. Rev. A **50**, 240 (1994).
[30] K. Burke, J.P. Perdew, and M. Ernzerhof, Int. J. Quantum Chem. **61**, 287 (1997).
[31] J. Tao, P. Gori-Giorgi, J.P. Perdew, and K. Schmidt, Bull. Am. Phys. Soc. **L24**.006 (2001).
[32] N.C. Handy and A.J. Cohen, Mol. Phys. **99**, 403 (2001).
[33] J.P. Perdew and Y. Wang, Phys. Rev. B **45**, 13244 (1992).
[34] M. Seidl and J.P. Perdew, in preparation.
[35] M. Lein, E. K. U. Gross, and J. P. Perdew, Phys. Rev. B **61**, 13431 (2000).
[36] In Refs. 12,14,26 the RPA spin-resolution is assumed exact for the long-range part of g_{xc} at all densities. Further studies by one of us (P.G.-G.) showed that this is true only when $r_s \to 0$, but with small deviations as r_s increases, so that the assumption made is still quite accurate at $r_s \sim 10$.
[37] This assumption is reasonable, but could be inexact. In the low-density limit, the electron gas becomes ζ-independent, since the statistics is irrelevant with respect to Coulomb repulsion, but magnetic order can be present, so that $g_{xc}^{\uparrow\downarrow}$ may differ from $g_{xc}^{\uparrow\uparrow}$ for $u/r_s \gtrsim 1$. A close comparison of our Figs. 1 and 8 for $r_s = 10^5$ and $\zeta = 0$ seems to show this effect. (For $u/r_s \lesssim 1$ both $g_{xc}^{\uparrow\downarrow}$ and $g_{xc}^{\uparrow\uparrow}$ tend to zero in the strongly correlated limit.)
[38] J. Tao, P. Gori-Giorgi, J.P. Perdew, and R. McWeeny, Phys. Rev. A **63**, 32513 (2001).
[39] J. C. Kimball, Phys. Rev. A **7**, 1648 (1973).
[40] K. Tatarczyk, A. Schindlmayr, and M. Scheffler, Phys. Rev. B **63**, 235106 (2001).
[41] P. Gori-Giorgi and P. Ziesche, cond-mat/0205342.
[42] B. Davoudi, M. Polini, R. Asgari, and M.P. Tosi, Phys. Rev. B **66**, 075110 (2002).
[43] M. Abramowitz and I. Stegun, *Handbook of Mathematical Functions* (Dover Publications Inc., New York, 1965).